



# LUND UNIVERSITY

## Thermal properties on high fill factor electrical windings: Infiltrated vs non infiltrated

Siesing, Leif; Reinap, Avo; Andersson, Mats

*Published in:*  
2014 International Conference on Electrical Machines (ICEM)

*DOI:*  
[10.1109/ICELMACH.2014.6960492](https://doi.org/10.1109/ICELMACH.2014.6960492)

2014

[Link to publication](#)

*Citation for published version (APA):*  
Siesing, L., Reinap, A., & Andersson, M. (2014). Thermal properties on high fill factor electrical windings: Infiltrated vs non infiltrated. In *2014 International Conference on Electrical Machines (ICEM)* (pp. 2218-2223). IEEE - Institute of Electrical and Electronics Engineers Inc.. <https://doi.org/10.1109/ICELMACH.2014.6960492>

*Total number of authors:*  
3

### General rights

Unless other specific re-use rights are stated the following general rights apply:  
Copyright and moral rights for the publications made accessible in the public portal are retained by the authors and/or other copyright owners and it is a condition of accessing publications that users recognise and abide by the legal requirements associated with these rights.

- Users may download and print one copy of any publication from the public portal for the purpose of private study or research.
- You may not further distribute the material or use it for any profit-making activity or commercial gain
- You may freely distribute the URL identifying the publication in the public portal

Read more about Creative commons licenses: <https://creativecommons.org/licenses/>

### Take down policy

If you believe that this document breaches copyright please contact us providing details, and we will remove access to the work immediately and investigate your claim.

LUND UNIVERSITY

PO Box 117  
221 00 Lund  
+46 46-222 00 00

# Thermal properties on high fill factor electrical windings: Infiltrated vs non infiltrated

L. Siesing, A. Reinap, M. Andersson

**Abstract** -- This paper presents a comparison of the thermal properties between infiltrated and non-infiltrated copper windings. The focus is on thermal conductivity in the radial direction on the winding. The samples have a fill factor above 65 % due to the manufacturing method of the samples. Samples are produced and measured with the transient plane source technique and then compared to FEM simulations and the Hashin and Shtrikman approximation. The results show a considerable difference between a non-infiltrated and an infiltrated winding, as well as a good agreement between measurements, FEM simulations and the Hashin and Shtrikman approximation.

**Index Terms**—Thermal analysis, Thermal conductivity, Coils, Winding, Fill factor, Infiltrated, Non-infiltrated

## I. INTRODUCTION

A major limiting factor when designing and exploiting any electromagnetic device is heat generation and dissipation in the winding. It is therefore important to have accurate data in the design step so that safety margins can be properly considered and performance increased. Moreover, accurate data, which includes the manufacturing data, makes it possible to design more effective and cheaper electromagnetic devices such as for example motors.

However, creating an accurate thermal model is difficult because thermal parameters differ depending on manufacturing methods and operating conditions. One of the more critical sets of parameters in electrical machine thermal modeling is the set describing the winding [1] [2] [3] [4]. The importance of this set is due to the large heat generation in the winding created by high current densities. A winding usually consists of a coated copper wire that is wound more or less thoroughly on a bobbin, around a pole or a tooth, etc. This means that a lot of air acts as an insulator, thereby decreasing the thermal conductivity drastically. Some windings are therefore infiltrated, impregnated or vanished to improve thermal conductivity.

Previously a problem regarding windings, both infiltrated and non-infiltrated is that the latter windings have been difficult to measure due to the lack of measuring methods that can perform this task with high accuracy. This study uses a Hot Disk 2500S which makes it possible to measure the thermal conductivity in the axial direction as well as in the plane, as long as the thermal conductivity is isotropic in the plane [5]. It is also possible to measure on non-infiltrated windings by using this equipment and thereby

performing measurements on the non-infiltrated samples and then infiltrate those with epoxy to get a proper comparison.

The experimental measurements are compared with a homogenization relation proposed by Hashin and Shtrikman [6] [7] [8], and to a finite element model of the used samples. This shows the difference between infiltrated and non-infiltrated windings and how well they correspond with measured data.

## II. METHOD

In order to be able to validate the results properly both FEA and an approximation are used in addition to the measured results. The methods are described in this chapter as well as the manufacturing of the test samples.

### A. Winding sample construction

A conventional enameled magnetic wire is used in the experimental work. The test samples are wound in a fixture that makes it possible to manufacture two at the same time. Two steel sheets are bent as a U and placed in the fixture with the backs facing each other. Copper wire is then wound inside the two U shaped steel sheets creating an almost oval shape. By then bending the excess steel sheet and compressing it, a compacted sample is created. At this point no binder is used, which in some cases makes the winding strands disengaged and sample instable and therefore has to be handled with care. High speed cutting and then polishing is performed to get a flat surface on one side of the sample, to place the measuring sensor on. A microscope picture of the polished surfaces for two samples can be seen in Fig. 1.

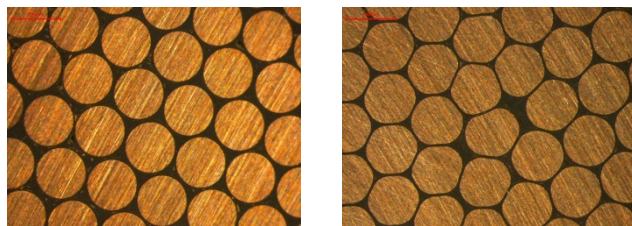


Fig. 1. Microscope picture of the polished surface of 74 % and 82 % fill factor, from left to right.

After measurement on the non-infiltrated windings, infiltration is performed. This is done by immersing the windings in epoxy and placing them in a vacuum chamber, to eliminate trapped air. The vacuum is released before the gelling starts. The surfaces are then polished before the new measurements are performed. Properties of the materials used when manufacturing the windings can be seen in table I.

This work was supported by FFI - Strategic Vehicle Research and Innovation, through the project Super cool.

L. Siesing and M. Andersson are with Division of Production and Material Engineering at Faculty of Engineering in Lund University, Sweden. Box 118, 22100 Lund, Sweden. (e-mail: leif.svensson@iprod.lth.se, mats.andersson@iprod.lth.se)

A. Reinap are with Division of Industrial Electrical Engineering and Automation at Faculty of Engineering in Lund University, Sweden. Box 118, 22100 Lund, Sweden. (e-mail: avo.reinap@iea.lth.se)

TABLE I  
PROPERTIES FOR THE MATERIALS USED IN THE WINDING.

	Copper	Polyamide imide	Epoxy
Thermal conductivity [W/mK]	385	0.26	0.21
Specific heat [MJ/m <sup>3</sup> K]	3.49	1.44	1.71
Density [kg/m <sup>3</sup> ]	8890	1440	1200
Conductor diameter [mm]	1, 0.3	na	na
Insulation thickness [mm]	na	0.035, 0.021	na

### B. Winding modeling

The model of the winding is made in a finite element analysis (FEA) tool as this is the most convenient way of taking the detailed geometry into account. A 2D FE heat transfer analysis in FEMM software is used to estimate the thermal conductivity of the winding. As the outcome of the FEA, the field distribution and the flows can be counted also in great details. A section of winding or a coil is drawn and solved for thermal steady state solver. The principal sketch of the model is shown in Fig. 2 and the governing equation system (1) and (2). In order to calculate an equivalent thermal conductivity inside a coil, a 1D heat flow is considered where the temperatures in the front and the back edge are defined and no heat exchange through the lateral sides are expected. Therefore, in order to define temperature difference across the analysis domain,  $\Delta\vartheta = \vartheta_2 - \vartheta_1$ , Dirichlet boundary condition of the given temperatures is defined on vertical edges:  $\vartheta_1 = 0^\circ\text{C}$  and  $\vartheta_2 = 10^\circ\text{C}$ . Neumanns boundary condition defines the heat flux through the surfaces and is assigned on the horizontal edges of the model. FE-mesh of linear triangular elements is used to discretize the model domain with moderate number of elements so that the heat flux distribution is clearly distinguishable. The important outcome of the model is obtaining the heat flow across the temperature difference. By calculating the heat flow and knowing the temperature difference, the thermal conductivity is calculated.

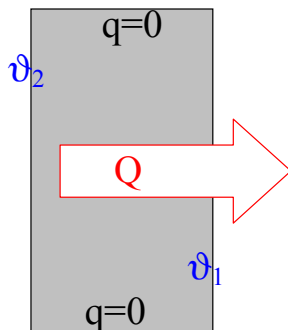


Fig. 2. Modelling setup in FEA.

$$G_{th} = \frac{kA}{l} = \frac{Q}{\vartheta_2 - \vartheta_1} = \frac{Q}{\Delta\vartheta} \quad (1)$$

$$k = \frac{Q}{\Delta\vartheta} \frac{l}{A} \quad (2)$$

As the dielectric insulation or the coating thickness depends on the wire diameter, the calculations are carried out for two different diameters of the sample wires, 1 mm and 0.3 mm, respectively.

The first group of figures (Fig. 3 and Fig. 4) shows 1mm wire with 0.035 mm coating with thermal conductivity of 0.26 W/mK. The thermal conductivity of filling material is varied from 0.02 to 1 W/mK. Fig. 3. shows the heat flux density for 0.03 W/mK (left, non-infiltrated) and 0.2 W/mK (right infiltrated) for the coil of 79% of fill factor or 1 $\mu\text{m}$  spacing between the wires.

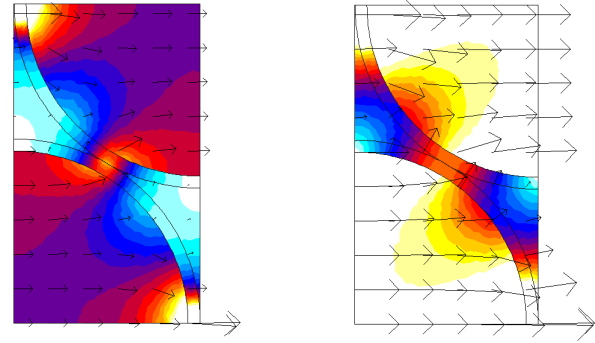


Fig. 3. FEA of the heat flux density in a winding segment for a 1 mm wire, with 1  $\mu\text{m}$  distance between wires. Left: the heat flux density for 0.03 W/mK (non-infiltrated); and Right: 0.2 W/mK (infiltrated).

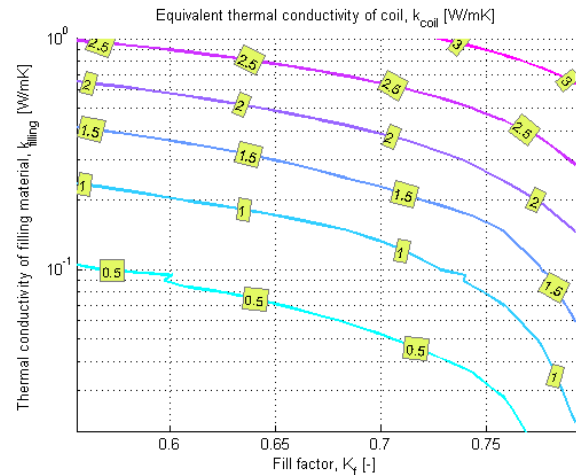


Fig. 4. FEA results for fill factor vs thermal conductivity of potting compound as well as the winding segment in total for a 1 mm wire.

It has to be noted that this fill factor does not take into account the edge effects and considers only the packing inside the coil.

The second group of figures (Fig. 5 and Fig. 6) shows 0.3mm wire with 0.0635 mm coating that has thermal conductivity of 0.26 W/mK. The thermal conductivity of filling material is varied from 0.02 to 1 W/mK. Fig. 5. shows the heat flux density for 0.03 W/mK (left, non-infiltrated) and 0.2 W/mK (right infiltrated) for the coil of 44.7% of fill factor or 1 $\mu\text{m}$  spacing between the wires.

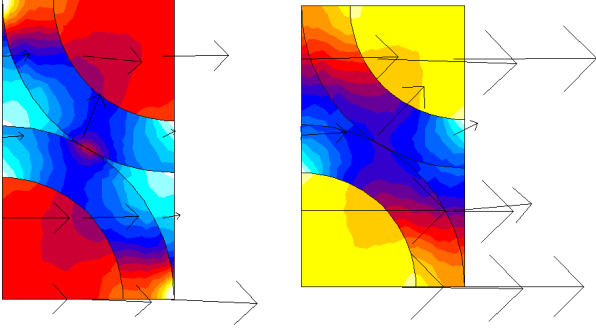


Fig. 5. FEA of the heat flux density in a winding segment for a 0.3 mm wire, with 1  $\mu\text{m}$  distance between wires. Left: the heat flux density for 0.03 W/mK (non-infiltrated); and Right: 0.2 W/mK (infiltrated).

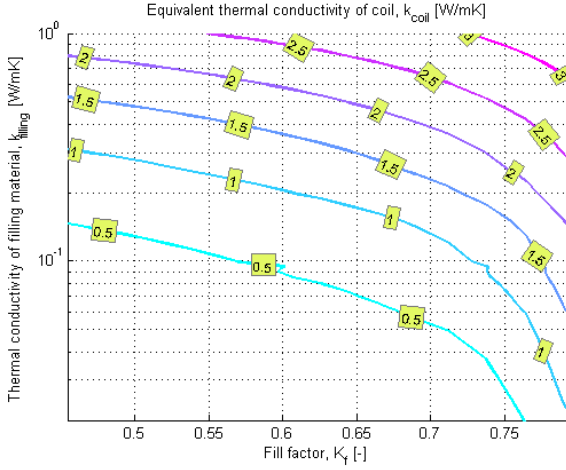


Fig. 6. FEA results for fill factor vs thermal conductivity of potting compound as well as the winding segment in total for a 0.3 mm wire.

All these previously obtained fill factors are based on increasing the distance between the coils in step of 20  $\mu\text{m}$ , from 1  $\mu\text{m}$  to 201  $\mu\text{m}$ .

### C. Thermal property measurement

There are numerous ways to measure thermal properties on a material, in this study the transient plane source method has been used. The reason for choosing this method is that it is possible to measure on non-infiltrated samples. The equipment used is a TPS 2500 S from Hot Disk AB and is chosen due to the possibility of measuring on short pulses, which makes it possible to measure on small samples.

The sensor consists of an electrically conducting pattern in the shape of a double spiral, which has been etched out of a thin nickel foil. The spiral is sandwiched between two thin sheets of an insulating material (Kapton), se Fig. 7.

When performing a measurement, the sensor is placed between two pieces of the sample. Both samples have to have a flat surface at least twice the diameter of the sensor. A current is then run through the double spiral. The current needs to be strong enough to increase the temperature of the sensor with several degrees. The resistance is at the same time measured and recorded as a function of time. It is therefore not necessary to introduce other sensors or heating sources that risk influencing the measurement.

The thermal conductivity equation used in the software assumes that the sample is infinitely large. It is therefore important to only use data collected before the boundaries

influence the measurement.

In these tests, the 5501 sensor (6.403 mm in radius) was used. This sensor was recommended from the chief science officer at Hot Disk AB due to the size of the sample and the anisotropic characteristic.

Because the samples were anisotropic, the volumetric specific heat ( $\text{MJ}/\text{m}^3\text{K}$ ) needed to be known. This was calculated with (3) and the results can be seen in table II.

$$C_V = C_{v, cu} \times \vartheta_{cu} + C_{v, pi} \times \vartheta_{pi} + C_{v, air} \times \vartheta_{air} \quad (3)$$

Where  $C_v$  and  $\vartheta$  are volumetric specific heat and volume fraction with the subscripts  $cu$ ,  $pi$  and  $air$  representing the copper, polyamide imide and air, respectively.

TABLE II  
CALCULATED VOLUMETRIC SPECIFIC HEAT FOR THE DIFFERENT SAMPLES.

Sample	Wire diameter [mm]	Volumetric specific heat [ $\text{MJ}/\text{m}^3\text{K}$ ]
74 % infiltrated	1	2.97
74 % non-infiltrated	1	2.82
82 % infiltrated	1	3.13
82 % non-infiltrated	1	3.10
70 % infiltrated	0.3	2.89
70 % non-infiltrated	0.3	2.68
81 % infiltrated	0.3	3.11
81 % non-infiltrated	0.3	3.10

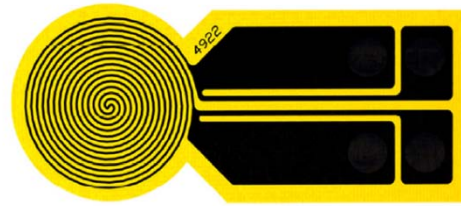


Fig. 7. Kapton sensor used for measurements.

### D. Hashin and Shtrikman approximation

The thermal conductivity of a winding segment can be estimated by the Hashin and Shtrikman approximation (4) if it only consists of two materials. Because of the small difference of material properties between the epoxy and the polyamide-imide on the copper wire, they are assumed to be one material. Also when there is no epoxy, but only air, the air and polyamide-imide are assumed to be one material. The thermal conductivity used in the approximation is therefore weighted depending on the percentage of the different materials.

$$k_e = k_p \frac{(1 + \vartheta_{cu}) \times k_{cu} + (1 - \vartheta_p) \times k_p}{(1 - \vartheta_{cu}) \times k_{cu} + (1 + \vartheta_p) \times k_p} \quad (4)$$

Where  $k$  and  $\theta$  are the thermal conductivity and volumetric fraction with the subscripts  $e$ ,  $p$  and  $cu$  representing the effective, potting and copper respectively.

### III. RESULTS AND DISCUSSION

The comparison between infiltrated and non-infiltrated windings can be seen in Table III, which shows that infiltration can result in similar increase in thermal conductivity compared to the increase in fill factor from 74 vol % to 82 vol %. However, infiltration is easier since to achieve 82 vol % fill factor requires high forces, thereby risking damaging the wires. Comparing the thermal conductivity of two coils with two different wire dimensions shows that the thinner wire results in higher thermal conductivity than the thicker, when non-coated, which is due to the higher amount of insulator material on the thinner wire causing a low amount of air in the structure.

It is however harder to use a smaller wire diameter

compared to a larger wire diameter when manufacturing a winding with the same fill factor. Due to the low thermal conductivity in the epoxy even when infiltrated, the thermal conductivity in the winding with thicker wire will be slightly lower than the thinner wire. It can though be seen in the measurements that the thicker wire has higher thermal conductivity. This is probably due to higher difficulty to infiltrate an already dense structure.

The results also show that the thermal conductivity in the axial direction is only marginally changed compared to its already high thermal conductivity. This is probably due to the high thermal conductivity in copper compared with the relatively low in air and epoxy. This difference is also dependent on the high percentage of copper compared to the other materials, meaning that a lower fill factor copper would increase the difference of thermal conductivity.

Fig. 8 shows a comparison between the Hashin and Shtrikman approximation and the measured data from infiltrated samples.

TABLE III  
THERMAL CONDUCTIVITY MEASUREMENTS.

	Fill factor [%]	Wire diameter [mm]	Thermal conductivity [W/mK]		Standard deviation	
			Radially	Axially	Radially	Axially
Non-infiltrated	74	1	0.79	293	0.10	13.23
	82	1	1.48	300	0.05	8.17
	66	0.3	0.67	252	0.06	8.26
	74	0.3	0.96	270	0.04	2.78
Infiltrated	74	1	1.47	290	0.02	14.20
	82	1	2.10	320	0.03	5.62
	66	0.3	1.03	250	0.04	18.92
	74	0.3	1.34	278	0.06	8.55

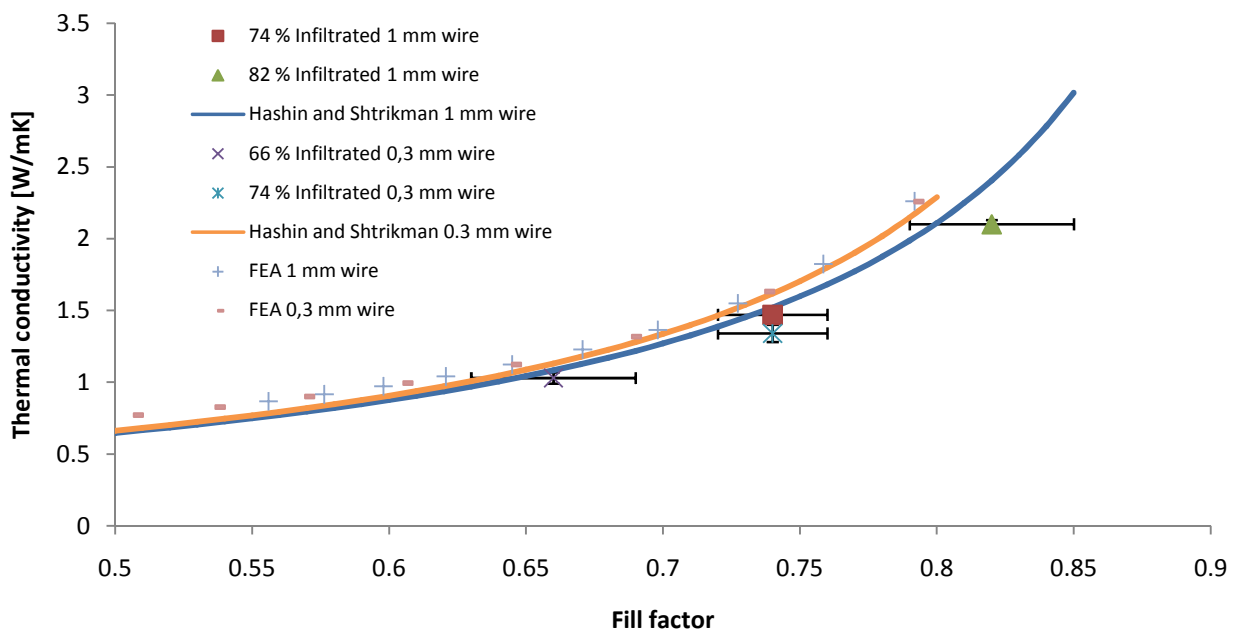


Fig. 8. Comparison of the Hashin and Shtrikman model with measured data from infiltrated samples.

Due to the restrictions of two materials in the Hashin and Shtrikman model a mean value, weighted by volume percent of insulator and epoxy, was used. It is clear from Fig. 8 that the model, that is an approximation, describes the measured value at 74 % well, whereas the value at 82 % is less well described.

The reason for this difference might be that even a small change in thermal conductivity of the insulation and epoxy materials in the model will have a much bigger impact at high fill factor than at a low. [4] assumed that the insulation material (0.26 W/mK) on the copper has sufficiently similar properties to the potting material (0.85 W/mK) and could therefore be used for calculation. Using the same approach in this study resulted in high thermal conductivity, which can be seen in Fig. 9. This same phenomenon could be observed in [4] especially at higher fill factors. This shows that even a small difference in material properties can affect the results and should not be neglected. Also the FEA is in good agreement with the measured results as well as the Hashin and Shtrikman approximation.

To be able to use the Hashin and Shtrikman model on non-infiltrated windings a mean value, weighted by volume of thermal conductivity between air and insulation, is used in Fig. 10. The figure shows good agreement between measured values and the approximation, which makes it possible to use the approximation even when there are relatively big differences in material properties, at least at high fill factors. The FEA are however not in good agreement with the measured results nor the approximation. This is due to the assumption that the wire is perfectly centered in the middle compared to the adjacent wires and heat transfer takes place only due to thermal conduction. Even though the geometric distance is very small from the adjacent strands the FE model considers that the wire is perfectly and evenly placed. This results that when the strand isolation is coming to contact with the adjacent wires the equivalent thermal conductivity of the winding is changing abruptly. Otherwise the low thermal conductivity of air determines the low thermal conductivity of the winding according to FEA (Fig. 10).

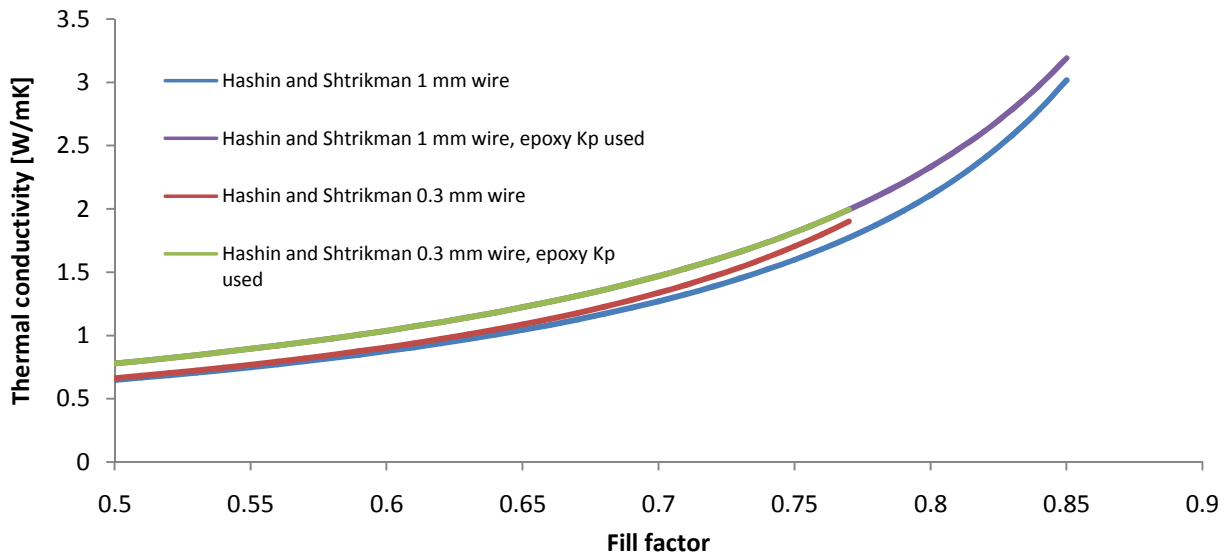


Fig. 9. Comparison of the Hashin and Shtrikman model with and without mean values of potting compound.

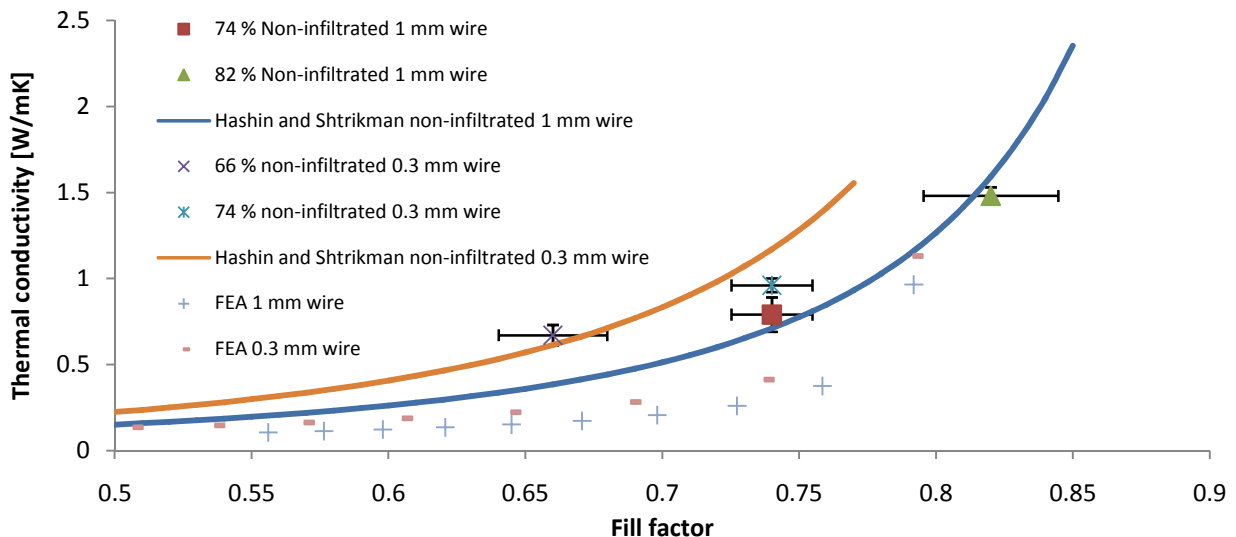


Fig. 10. Comparison of Hashin and Shtrikman with measured data from Non-infiltrated samples.

To be able to use the Hashin and Shtrikman model on non-infiltrated windings a mean value, weighted by volume of thermal conductivity between air and insulation, is used in Fig. 10. The figure shows good agreement between measured values and the approximation, which makes it possible to use the approximation even when there are relatively big differences in material properties, at least at high fill factors. The FEA are however not in good agreement with the measured results nor the approximation. This is due to the assumption that the wire is perfectly centered in the middle compared to the adjacent wires and heat transfer takes place only due to thermal conduction. Even though the geometric distance is very small from the adjacent strands the FE model considers that the wire is perfectly and evenly placed. This results that when the strand isolation is coming to contact with the adjacent wires the equivalent thermal conductivity of the winding is changing abruptly. Otherwise the low thermal conductivity of air determines the low thermal conductivity of the winding according to FEA (Fig. 10).

#### IV. CONCLUSION

Comparisons between measured results and calculated results in form of the Hashin and Shtrikman approximation and a FEA have been performed. The results show good agreement between the Hashin and Shtrikman approximation and the measured results. There is however different results obtained from FEA. As a matter of fact Hashin and Shtrikman approximation bases on two materials and their volumetric differences, FEA on contrary considers the exact geometry and materials over the model domain. This exactness in FEA becomes the limitation as in the reality the winding strands are not perfectly placed, the material deviations and geometric tolerances the influences the outcome.

It is however evident that there are a significant difference in thermal conductivity between non-infiltrated and infiltrated windings. To get a good picture of the magnitude of the windings impact on the motor design, a study on a whole motor model is necessary.

#### V. REFERENCES

[1] A. Jack, B. Mecrow, P. Dickinson, D. Stephenson, J. Burdess, N.

- Fawcett och J. and Evans, "Permanent magnet machines with powdered iron cores and pre-pressed windings," i *IAS'99*, Phoenix, 1999.
- [2] R. Wrobel, P. Mellor och a. D. Holliday, "Thermal modeling of a segmented stator winding design," *IEEE Trans. Ind. Appl.*, vol. 47, nr 5, pp. 2023-2030, 2011.
- [3] M. Galea, C. Gerada, P. Wheeler och T. Raminosa, "A thermal improvement technique for the phase windings of electrical machines," *IEEE Trans. Ind. Appl.*, vol. 48, nr 1, pp. 79-87, 2012.
- [4] N. Simpson, P. H. Mellor och R. Wrobel, "Estimation of equivalent thermal parameters of electrical windings," *IEEE Trans. Ind. Appl.*, vol. 49, nr 6, pp. 2505-2515, 2013.
- [5] "22007-2:2008, ISO, Plastics -- Determination of thermal conductivity and thermal diffusivity -- Part 2: Transient plane heat source (hot disc) method".
- [6] L. Idoughi, X. Mininger, F. Bouillault, L. Bernard och a. E. Hoang, "Thermal model with winding homogenization and fit discretization for stator slot," *IEEE Trans. Magn.*, vol. 47, nr 12, pp. 4822-4826, 2011.
- [7] C. P. Steinmetz, "On the law of hysteresis," *AIEE Transactions*, vol. 9, nr 1, pp. 3-64, 1892.
- [8] L. Corcolle och R. Daniel, "A note on the effective magnetic permeability," *IEEE Trans. Magn.*, vol. 43, nr 7, pp. 3153-3158, 2007.

#### VI. BIOGRAPHIES

**Leif Siesing (former Svensson)** was born in Sweden in 1982. In 2009 he graduated as a MSc. on Mechanical Engineering from the Faculty of Engineering of Lund University. Currently, he is a PhD student at the Division of Production and Material Engineering, at the Faculty of Engineering of Lund University (LTH) in Sweden.

**Avo Reinap** was born in Estonia in 1973. He received the Diploma in Engineering and the MSc degrees in Power Engineering from Tallinn University of Technology, Estonia, in 1998 and 2000, respectively. He received the PhD degree in technology from Lund University, Sweden, in 2005. From 2005 to 2010 he was an Associate Professor in the Department of Electrical drives and Power Electronics in Tallinn University of Technology and from 2007 to 2011 a postdoctoral fellow in the Department of Industrial Electrical Engineering and Automation at the Faculty of Engineering of Lund University.

**Mats Andersson** is currently associate professor in Department of Production and Materials Engineering, Lund University and has specialized in process dynamics in machining operations, with a special focus on the interaction between chip formation, machined surfaces, tool geometries and process damping. In the metal cutting area, he has also established an expertise in force measurement systems for metal cutting, especially for measuring of high frequency cutting forces. In addition to this, he has played an active part in the ongoing development of new manufacturing techniques for high performance flux conductors based on soft magnetic composites.